Immunity, Volume *38*

Supplemental Information

Recruitment of Beneficial M2 Macrophages to Injured Spinal Cord Is Orchestrated by Remote Brain Choroid Plexus

Ravid Shechter, Omer Miller, Gili Yovel, Neta Rosenzweig, Anat London, Julia Rist, Ki-Wook Kim, Eugenia Klein, Vyacheslav Kalchenko, Peter Bendel, Sergio A. Lira, Steffen Jung, and Michal Schwartz

Inventory of Supplemental Information

Supplementary Data:

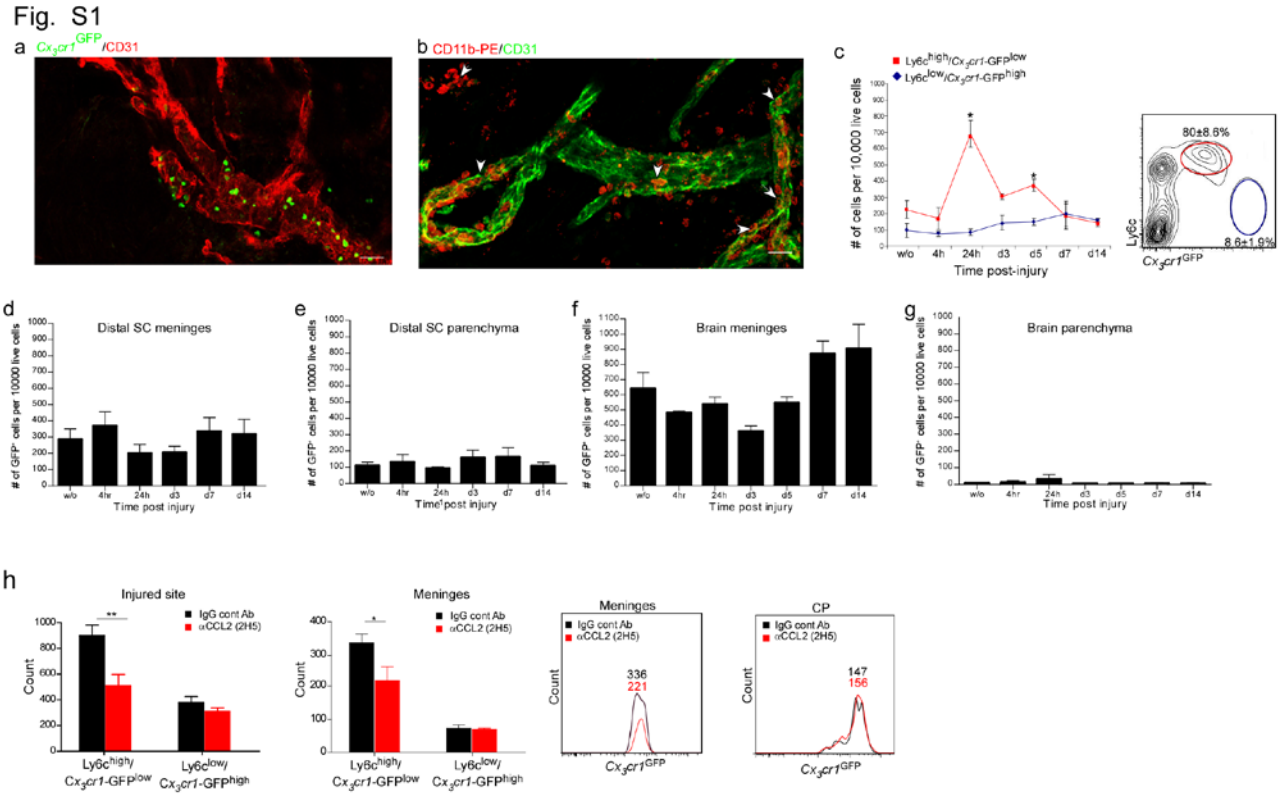

Figure S1, related to Figure 2. (**a,b**) Confirmation of monocyte arrival to the spinal cord leptomeninges following spinal cord injury in the non chimeric model. (a) Representative picture of whole mount of leptomeninges of C57BL/6 mice that were spinally injured, intravenously injected 4 hours later with monocytes (*Cx3cr1*$^{GFP/+}$), and dissected out 1 day later (n=7 mice were analyzed). (b) Homing monocytes were visualized via their *in-situ* labeling by intravenously injected PE-conjugated anti-CD11b antibodies (intravenously injected 1 day before the injury); representative pictures of whole mounts of excised spinal cord leptomeninges (1 day post-injury) are shown (n=5 mice, two repetitions). (**c**) Representative topographical maps, and quantitative analysis of monocyte characteristics in the spinal cord meninges of *Cx3cr1*$^{GFP/+}$ chimeras, according to Ly6c and *Cx3cr1*$^{GFP/+}$ expression (n=3-8 mice for each time point); *two-way ANOVA*; ι- F=9.6. * relative to the relevant subset in non-injured animals (w/o). (**d-g**) Monocytes do not accumulate at other potential CNS entry sites following spinal cord injury. *Cx3cr1*$^{GFP/+}$ chimeras were subjected to spinal cord injury. At different time points following injury, the covering leptomeninges of the spinal cord parenchyma located 0.5 cm distally to the lesion site (d), and the underlying parenchyma (e), as well as the cerebral leptomeninges (f), and dissected parts of their brain parenchyma (g) were quantified by flow cytometry for GFP$^+$ cells. n=3-4 mice per time point. *ANOVA*; d- $F_{5,13}$=1.04, p=0.418; e- $F_{5,13}$=0.603, p=0.699; f- $F_{6,15}$=5.065, p=0.005; g- $F_{6,14}$=0.957, p=0.487; none of the time points were significantly different relative to uninjured (w/o). (**h**) Injured *Cx3cr1*$^{GFP/+}$ chimeras, intraperitoneally injected with anti-CCL2 (or isotype matched IgG) antibodies, analyzed by flow cytometry on d5 for GFP$^+$ cells in their excised SC leptomeninges, lesion sites and choroid plexus. CCL2 inhibition impaired Ly6c^{high}/*Cx3cr1*-GFP^{low} trafficking to the injured site and leptomeninges (*two-way ANOVA*; n=4-5mice; Injured site- P=0.0042, F=12.39; meninges- P=0.036, F=5.54). Values are absolute cell numbers in 0.5 cm SC tissue. Histograms for GFP in the leptomeninges and CP, of control and CCL2 treated mice, are shown; cells were pre-gated according to CD11b/Ly6c. Data are represented as mean +/- SEM. Scale bar representation: 100µm.

Fig. S2

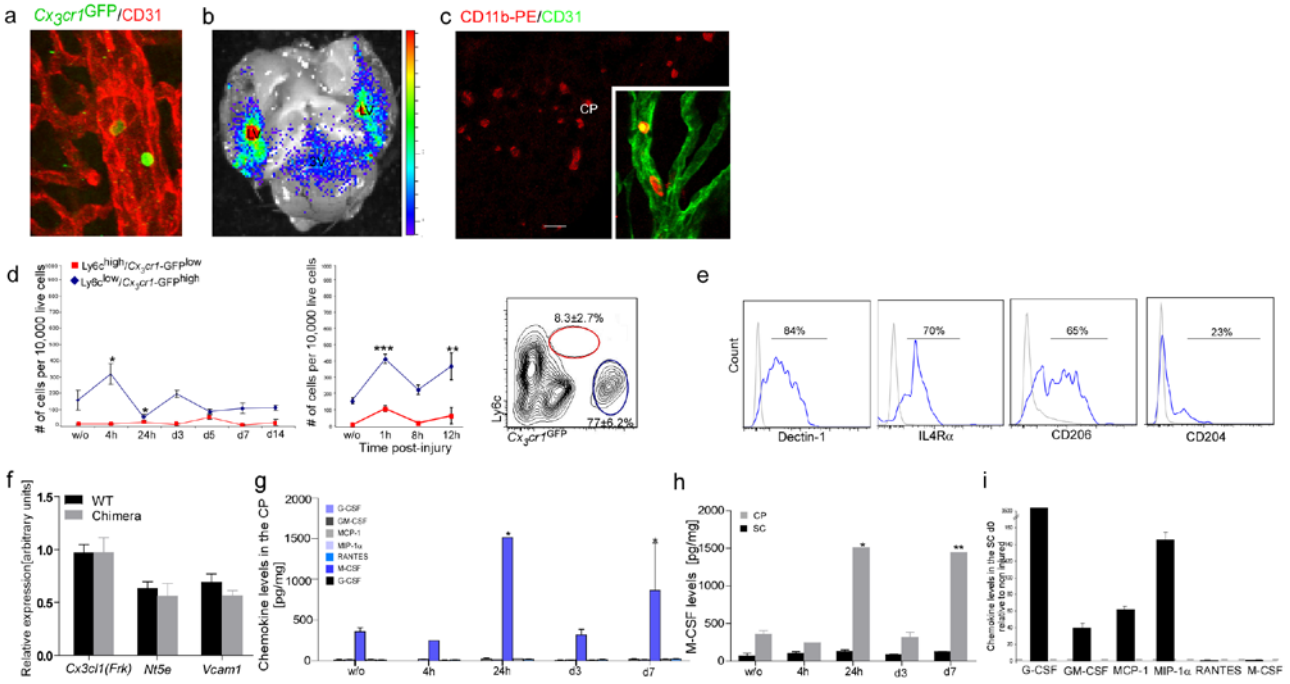

Figure S2, related to Figure 3. (a-c) Validation of post injury monocyte infiltration to the choroid plexus in a non-chimeric model. (a) Representative pictures of whole mounts of choroid plexus of spinally injured wt mice that were intravenously injected (4-5 hours prior to their excision) with *Cx$_3$cr1*$^{GFP/+}$ monocytes (CP were excised 8 hours after the injury; n=7 mice were analyzed). (b) Color-coded near-infrared fluorescent image overlaid on a photographic image of an isolated brain, in which the lateral ventricles are exposed, taken from a recipient of DiR-labeled monocytes (cells were injected approximately 4 hours after the injury; one mouse is shown, representative of three analyzed). (c) Representative pictures of whole mounts of CP (excised 1 day post-injury) following *in-situ* labeling of circulating myeloid cells by intravenously injected PE-conjugated anti-CD11b antibodies (injected 1 day before the injury) (n=5 mice, two repetitions). (**d**) Representative topographical maps, and quantitative analysis of monocyte characteristics and kinetics in the choroid plexus of *Cx$_3$cr1*$^{GFP/+}$ chimeras, according to Ly6c and *Cx$_3$cr1*$^{GFP/+}$ expression (n=3-8 mice for each time point); *two-way ANOVA* F=12.9, p=0.0001; F=3.3, p=0.03; * relative to the relevant subset in non-injured animals (w/o). (**e**) M2 markers expression (Dectin-1, IL-4Rα and Mannose receptor; CD204 as control) by GFP$^+$ Ly6c^{low} cells at the choroid plexus of injured *Cx$_3$cr1*$^{GFP/+}$ chimeras, as assessed by flow cytometry. Pooled samples of n=12 mice. (**f**) Expression of Fractalkine, CD73 and VCAM-1 by the choroid plexus is not affected by BM chimerism when created using head shielding. Choroid plexuses were excised from C57BL/6 mice and from *Cx$_3$cr1*$^{GFP/+}$ chimeras 2 months after bone marrow transplantation following irradiation using head protection. Quantitative real time PCR for the expression of *Cx$_3$cl1 (Fractalkine)*, *Nt5e* (CD73 gene) and *Vcam1*. Results are presented in arbitrary units, and normalized to the expression of the housekeeping gene, *Ppia* (n=4 mice per group, *Two-way* ANOVA, F(1,15)=0.68, p=0.43). (**g-i**) Differential myeloid chemokine profiles expressed at the lesion site and the choroid plexus. Dissected CPs and lesioned spinal cords from C57BL/6 mice were pooled (CP-from six mice; SC-from three mice) and evaluated by Multiplex analysis for a range of myeloid-specific chemoattractants. The results are presented as absolute protein levels per mg tissue (g,h), or as fold change in (i). *Two way ANOVA;* n=3 pools; g-F=3.61 p=0.0002 F_{cyto}=31.6 p<0.0001 F_{day}=5.61 p=0.001; h-F=107 p<0.0001; *ANOVA* i-F=21200 p<0.0001. Data are represented as mean +/- SEM. Scale bar representation: (b) 200µm; (a,c) 10µm.

Fig. S3

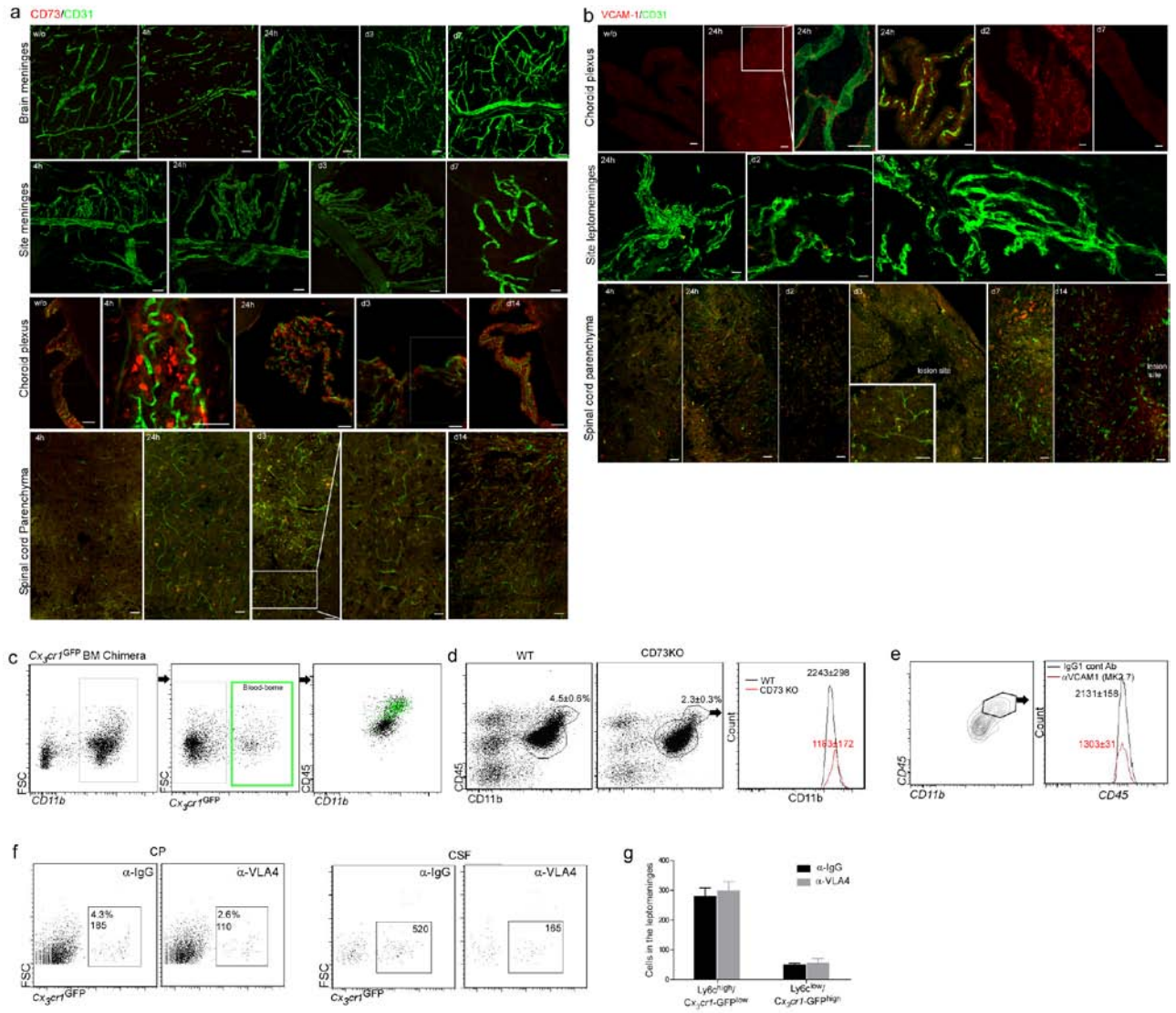

Figure S3, related to Figure 4. (**a,b**) CD73 and VCAM-1 are predominantly expressed within the CNS in the choroid plexus. Representative confocal images of isolated brain and spinal cord meninges, as well as choroid plexus and spinal cord sections, immunostained for either CD73 (a) or for VCAM-1 (b) together with CD31 (n=3-4 mice per time point; uninjured, 4h, 24h, days 2, 3, 7, 14 post-injury). No reactivity against CD73 was detected in either the vasculature of the meninges or parenchymal blood vessels. In contrast, intense staining was detected in the epithelial lining of the choroid plexus. While VCAM-1 immunoreactivity was observed in the vasculature of the choroid plexus at the early time points following injury, no significant reactivity was detected in either the vasculature of the meninges or parenchymal blood vessels. Sections from CD73 KO mice were used to verify CD73 staining. (**c-e**) Verification of inhibition of monocyte infiltration by interference with CD73 and VCAM1, as measured based on CD11b/CD45 levels in SC tissues following injury. (c) *Cx$_3$cr1*$^{GFP/+}$ chimeras were subjected to spinal cord injury and their spinal cord tissues were analyzed by flow cytometry. Infiltrating GFP$^+$ monocytes were CD11b^{high}/CD45^{high}, verifying the use of CD11b and CD45 for evaluating monocyte infiltration, and showing that all GFP$^+$ cells in our models correspond to infiltrating monocytes and not resident microglia (CD11b^{low}/CD45^{low}). (d) Decreased myeloid infiltration (CD11b^{high}/CD45^{high}) to the lesion site of CD73 knockout mice, as measured by flow cytometry 1 week after injury (*Student's t-test,* n=*3-4* mice per group, p=0.02). The histograms show the number of cells in 0.5cm SC tissue per 50,000

total live cells, pre-gated on $CD11b^{high}/CD45^{high}$ cells. (e) Administration of blocking antibody to VCAM-1 (d0,d2) decreases myeloid infiltration ($CD11b^{high}/CD45^{high}$) to the lesion site at d5 post injury in non-chimeric mice, measured by flow cytometry (*Student's t-test*, n=3-4 mice per group, p=0.006). The values presented in the histograms are the number of cells in 0.5cm SC tissue per 20,000 $CD11b^{+}$ cells, pre-gated on the infiltrating cells. One representative experiment out of two is shown. (**f**) Pooled samples of CPs and aspirated CSF, following treatment of injured chimeras with anti-VLA-4 or control anti-IgG, were analyzed for infiltrating GFP^{+} cells. The values for CSF samples represent cells in 100 μl. (**g**) Spinal cord leptomeninges samples of injured chimeras, following treatment with anti-VLA-4 or control anti-IgG antibodies, were analyzed by flow cytometry for infiltrating GFP^{+} cells (0.5cm SC tissue), and their subsets according to Ly6c and $Cx_3cr1^{GFP/+}$ expression (n=3-4 mice in a group; 2 way *ANOVA* F=0.087; P=0.77). Data are represented as mean +/- SEM. Scale bars: (a) 100μm; (b, a-spinal cords) 50 μm; (enlargements) 20 μm.

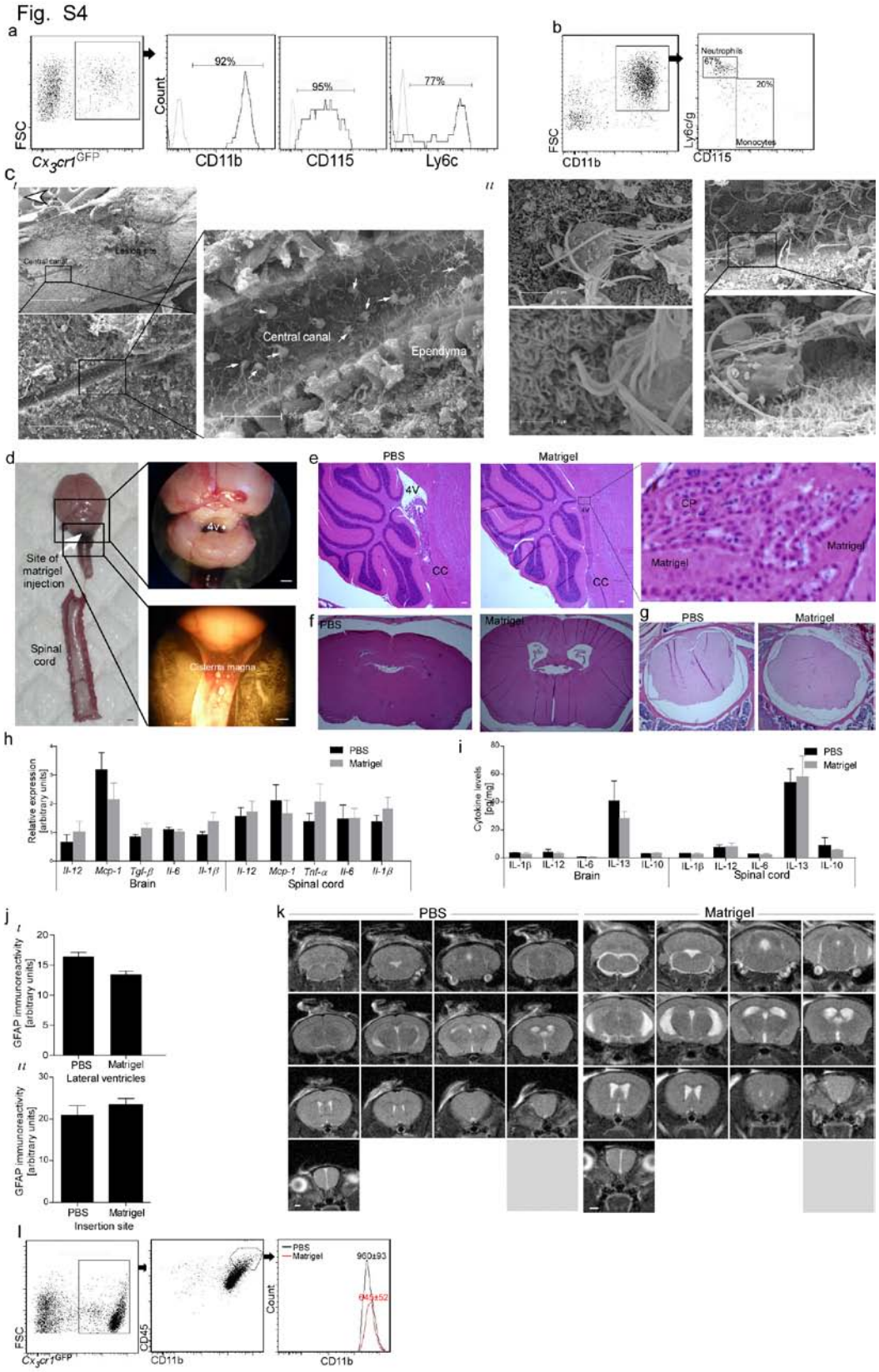

Figure S4, related to Figure 6. (**a,b**) Characterization of cells in the CSF post injury. A pooled CSF sample aspirated from the cistern magna of injured non-chimeric *Cx$_3$cr1*$^{GFP/+}$ mice or injured C57BL/6 mice (both 24h post-injury, n=8-12 mice per staining), assessed by flow cytometric analysis for monocytic markers (a), or neutrophils (b), respectively. Representative data from three repetitions are shown. (**c**) Scanning electron-microscopy revealing cells reminiscent of leukocytes

within the central canal. (*ι*)Scanning electron microscopy (SEM) of exposed central canal of wild type injured mice (day 7 post injury), identified by its cuboidal ependymal lining. (*ιι*) High magnification of central canal-associated cells reminiscent of leukocytes. Central canal associated cells were found to exhibit bundled filopodia, which were observed to make contact with the lining of the central canal, or formed connections between cells. N=3-5 mice; repeated 3 times. (**d-k**) Validation of the Matrigel administration used for obstruction of CSF flow. Wild type noninjured mice were cisternally injected with Matrigel or PBS and were evaluated for Matrigel deposition, the creation of hydrocephalus, and for signs of inflammation. (d) Photograph of brain following injection of Matrigel mixed with ink. (e-g) Representative histological images of brain sagital sections of the 4th ventricle (e), of whole head cross sections, including the lateral ventricles (f), or of spinal column cross sections (g) from PBS and Matrigel injected mice, 1 week post injection (n=7 mice per group; repeated twice). Hematoxylin and Eosin staining is shown. To preserve the leptomeninges, entire heads/spinal columns were imbedded. (h) Quantitative real time PCR for an array of cytokines tested in the brain and the spinal cord parenchyma assessed 1week after injection (presented in arbitrary units and normalized to a housekeeping gene; n=4 mice per group, *Two-way* ANOVA, Brain- $F(1,26)=0$, $p=0.99$, spinal cord- $F(1,22)=0.45$, $P=0.51$). (i) Multiplex analysis of cytokines in extract of brain and spinal cord parenchyma of the two groups 1 week after the injection (n=3 pools of three mice in each group, *Two-way* ANOVA, spinal cord-$F(1,15)=0$, $p=0.98$, brain- $F(1,15)=1.2$, $p=0.29$). (j) GFAP immunoreactivity in the parenchyma adjacent to the lateral ventricles including the hippocampus (ι), and in the parenchyma surrounding the insertion site (ιι) (*Student's t-test*, (ι) $p=0.1$, (ιι) $p=0.42$). (k) T2-weighted magnetic resonance images, performed on live mice 1 week after cisternal injection (PBS or Matrigel), showing coronal slices. Cerebrospinal fluid appears bright (n=9-15 per group, repeated four times). (**l**) Monocyte recruitment (evaluated according to the $CD11b^{high}/CD45^{high}$ population) to the lesion site following Matrigel administration was analyzed by flow cytometry, in non-chimeric mice. Matrigel injection resulted in reduced monocyte infiltration to the lesion site (*Student's t-test*, n=5-7 mice, $p=0.02$; one representative experiment out of three). The values in the histograms represent the absolute number of positive cells per 0.5cm length spinal cord tissue. Data are represented as mean +/- SEM.

Supplemental Experimental Procedures

Bone marrow radiation chimeras.

Bone marrow (BM) chimeras were prepared as previously described (Shechter et al., 2009). In brief, chimeras were prepared by subjecting gender-matched recipient mice to lethal whole-body irradiation (950 rad) while shielding the head. The mice were then reconstituted with 5×10^6 BM cells. The mice were left untouched to enable reconstitution of the hematopoietic lineage for 8-10 weeks after BM transplantation, prior to the experiments. The percentage of chimerism was determined in the blood according to percentages of GFP or CD45.1 expressing cells out of circulating monocytes (CD115). In this head-shielded model, an average of 50% chimerism was achieved. We found that shielding prevented infiltration of GFP^+ myeloid cells (microglial turnover) to the uninjured spinal cord (Shechter et al., 2009). Here, we further evaluated this model to show that the GFP fluorescence seen following SCI is entirely $CD45^{hi}/CD11b^{hi}$, representing monocytes and not microglia (**Fig. S3**). We previously demonstrated that this model, created while shielding the brain, preserves the physiological recruitment and homing of monocytes following SCI(Shechter et al., 2009). In each experiment, mice with comparable blood chimerism were chosen. The results were routinely normalized to the individual percentage of chimerism measured in the blood (a normalization factor was defined as [f=50/ percentage of chimerism]).

Assessment of functional recovery

Spinal cord injured mice were maintained on twice-daily bladder expression. Recovery was evaluated by hind-limb locomotor performance, assessed according to the open-field Basso Mouse Scale (BMS) (Basso et al., 2006), as previously described (Shechter et al., 2009). In this scale, a nonlinear score ranging from 0 (complete paralysis) to 9 (normal mobility) is assigned, and each possible score represents a distinct motor functional state. Mice were randomly assigned to groups prior to treatment, while validating similar average starting functional score, evaluated on 24h post injury, between groups. Notably, motor skill during the first day (d0) does not reflect the insult severity or the healing mechanism, but is a reflection of a spinal shock; therefore animals are not scored on the day of injury, but 24 hours later. Blinded scoring ensured that observers were not aware of the identity of tested animals. Locomotor function in an open field was monitored twice a week by placing the mouse for 4 min at the center of a circular enclosure (diameter 90cm, wall high 7 cm) made of molded plastic with a smooth nonslippery floor. Animals that showed a difference of more than 2 score points between their two hind limbs were excluded from the analysis. The

recovery observed is consistent with our many previous reports (Shechter et al., 2009), and those of others using moderate SCI(Donnelly et al., 2011). For details regarding lesion size evaluation, please see the "histology" section, below, of the Supplementary Information.

CSF collection. CSF was collected by the cisterna magna puncture technique. In brief, mice were anesthetized and placed on a stereotactic instrument so that the head formed a 135° angle with the body. A sagittal incision of the skin was made inferior to the occiput, the subcutaneous tissue and muscle were separated, and a capillary was inserted into the cisterna magna through the dura matter lateral to the arteria dorsalis spinalis. Approximately 5µl CSF could be aspirated from an individual mouse, and therefore pooled samples from 9-12 animals were analyzed. In each experiment, equivalent volumes were analyzed from each group, and the results were normalized to a 100µl volume (normalization factor f=100/volume analyzed). Experiments were repeated, and the statistics of the replication are provided, without considering animal numbers in the pools.

Administration of blocking antibodies. LE/AF antibodies were used as previously described. A rat monoclonal antibody to VLA-4 (PS/2; Southern Biology; 50µg/mouse, intravenously(Kanehiro et al., 2000)), to VCAM-1 (M/K 2.7; Bio Express; 200µg/mouse, intravenously(Pereira et al., 2009)), and to CD11b (M1/70; Bio Express; 100µg/mouse, intravenously (Auffray et al., 2007)), or hamster IgG to CCL2 (2H5; Bio Express; 100µg/mouse, intraperitoneally (Getts et al., 2008)) were injected twice (d0 and d2; based on the previously reported antibody clearance rates). Isotype matched antibody (Rat IgG2b, Rat IgG1, or Hamster IgG, respectively) served as a control, according to the manufacturer's recommendation (Bio Express).

Labeling of circulating leukocytes.

The blood circulating leukocytes were stained by intravenous injection of CFSE (Invitrogen) 24h before the injury, as previously described (Ristevski et al., 2003). For visualization of blood-recruited myeloid cells, the previously described *in-vivo* pulse-labeling procedure was followed (Chiang et al., 2007), which entails intravenous injection of low doses of fluorophore-conjugated monoclonal antibody to selectively label hematopoietic cells in the vascular compartment, and to distinguish them from parenchymal cells. Mice were injected with 2 µg PE-conjugated anti-CD11b (eBioscience) in 200µl PBS, as previously described (Chiang et al., 2007). About 24-48h were

allowed to elapse before tissue dissection, in order to maximize antibody binding, and clearance of unbound label from the circulation.

Adoptive transfer of isolated monocytes. $CD115^+$ monocytes were isolated as previously reported (Shechter et al., 2009). Briefly, BM cells were harvested from the femur and tibiae of naïve mice, and enriched for mononuclear cells on a Ficoll density gradient. The $CD115^+$ BM monocyte population was isolated by MACS enrichment using biotinylated anti-CD115 antibodies and streptavidin-coupled magnetic beads (Miltenyi Biotec) according to the manufacturer's protocols. Monocyte purity in the graft was routinely checked by flow cytometry based on CD115 reactivity (purity of 85-90% was routinely observed); injected cells were predominated by $Ly6C^{High}$ (about 80-90%). For intravenous injections, 3.5×10^6 cells per mouse were used; for ICV administration, 0.5×10^6 cells per mouse were used. For the experiment using pertussis toxin, cells were treated as previously described (Geissmann et al., 2003).

Whole mount staining and immunohistochemistry.

All mice used for staining procedures and confocal imaging were transcardially perfused with PBS prior to tissue fixation. Choroid plexus was isolated from all brain ventricles. Spinal leptomeninges were separated from the spinal cord parenchyma, about 0.5 cm around the site of injury, and another piece was removed about 0.5 cm rostral to the site of injury. Brain leptomeninges covering the upper part of the brain were separated from the brain and skull. For whole mount choroid plexus and meninges, isolated tissues were fixed with 2.5% paraformaldehyde (PFA) for several hours, and subsequently transferred to PBS containing 0.05% sodium azide. Prior to staining, the dissected tissues were washed and blocked (20% horse serum, 0.3% Triton X-100, and PBS) for 1h at room temperature, with shaking. Whole mount staining with primary (in PBS containing 2% horse serum and 0.3% Triton X-100) or secondary antibodies (in PBS), was performed for 1h at room temperature, with shaking. Each step was followed by three washes in PBS. The tissues were applied to slides, mounted with Immu-mount (9990402, from Thermo), and closed with cover-slips. For staining of sectioned spinal cord and brains, two different tissue preparation protocols (paraffin embedded and microtomed frozen sections) were applied, as previously described (Shechter et al., 2009; Ziv et al., 2006). The following primary antibodies were used: rabbit anti-GFP (1:100; MBL); rat anti-CD31 (PECAM-1; 1:100; BD Bioscience); rabbit anti-glial fibrillary acidic protein (GFAP; 1:100; Dako Cytomation); mouse anti-TGFβ (1:200; R&D systems); rabbit anti-CD73 (1:50; Abcam); chicken anti-vimentin (1:1000; Millipore); rat anti-pan-endothelial cell antigen (MECA-32; 1:10,); mouse anti-cytokeratin (1:100; Covance); goat anti-transthyretin (1:50; Acris);

rat anti-reticular fibroblast (ER-TR7; 1:100; Abcam); rabbit anti-VCAM-1 (1:50; Santa-Cruz); mouse anti-stromal-derived factor-1 (SDF-1) (1:50; R&D Systems Inc., Minneapolis); and rat anti-ICAM-1 (1:100; Abcam). For tight junction staining, the following primary antibodies were used: mouse anti-ZO-1, and mouse anti occludin (1:100; Invitrogen). For microglial/MΦ labeling, TRITC- conjugated *Bandeiraea simplicifolia* isolectin B4 (IB-4; 1:50; Sigma-Aldrich) was added for 1 h to the secondary antibody solution. Secondary antibodies included: Cy2/Cy3-conjugated donkey anti-rat antibody and Cy3 conjugated donkey anti-mouse, goat or rabbit (1:200; all from Jackson Immuno Research). The slides were exposed to Hoechst stain (1:4,000; Invitrogen Probes) for 1 min. Two negative controls were routinely used in immunostaining procedures, staining with isotype control antibody followed by secondary antibody, and staining with secondary antibody alone. For CD73 immunostaining, knockout mice were used for verification of staining specificity. The N stated in the figure legends represents the number of animals analyzed in each group; all the tested animals from each group gave the same qualitative results. For microscopic analysis, a fluorescence microscope (E800; Nikon) or laser scanning confocal microscope (Carl Zeiss, Inc.) were used.

Myelin integrity was qualitatively examined on paraffin-embedded sections that were stained with Luxol/Nissl. For lesion size evaluation, three equivalent depths of longitudinal sections (coronal/frontal plane) were analyzed in each tested animal; the average is presented. Lesion sizes were determined automatically with Image-Pro Plus 4.5 software (Media Cybernetics) in μm (and are represented as mm^2), by an operator who was blinded to the identity (treatment group) of the sections. Sections from an additional depth were analyzed in a blinded manner by a histologist from the pathological unit of Weizmann Institute, at very high resolution by using a Nikon DS-Ri1 camera at a resolution of 1280x1024 fine, and quality 4076x3116 fine, 8bit. Similar lesion sizes were observed in our previous publications (Shechter et al., 2009), and in many others, using the same model with injury of similar severity.

Brain sections including ventricular CPs were stained by the pathological unit with Cresyl violet. A veterinary pathologist evaluated representative pictures taken from n=3 mice from each group (non injured, 4hr, do, d1, d3, d7). His evaluation is indicated in the text.

1 week following Matrigel injection, whole heads and spinal columns of Matrigel or PBS injected mice were embedded in order to define any resulting changes with respect to the parenchyma, the surrounding meninges, and skull/columns. Histological sections, H&E stained, of brain and spinal cords, which included meninges, site of needle insertion, and ventricles were examined by

veterinary pathologist who determined that there were no signs of inflammation as an outcome of the treatment.

Isolation of cells for flow cytometric analysis.

Prior to tissue collection, mice were perfused with PBS via the left ventricle. Blood and spinal cord tissues were treated as previously described (Shechter et al., 2009). For spinal cord analysis, pieces of 0.5cm length (for each sample) containing the lesion site in the middle, were used. Choroid plexus tissues were isolated from lateral, 3rd and 4th ventricles. Choroid plexus tissues were manually homogenized by pipetation or by mashing. Spinal meninges were separated from the spinal cord parenchyma (site meninges: about 0.5 cm around the site of injury; distal: another piece of 0.5 cm length rostral to the site of injury). Brain meninges covering the upper part of the brain were separated from the brain parenchyma and skull. Meninges were manually homogenized by mashing. For the kinetic experiments, spinal cord parenchyma, after removal of meninges, was used. For CSF analysis, freshly aspirated samples were pooled due to the limited volume (5µl) obtained from each single animal; pooled samples were used from 9-12 mice. In each experiment, equivalent CSF volumes were analyzed between groups, and the results were normalized to a 100µl volume (normalization factor f=100/volume analyzed). In all cases, samples were stained according to the manufacturers' protocols. All samples were filtered through an 80µm nylon mesh and blocked with Fc CD16/32 (1:100; BD Biosciences). The following fluorochrome-labeled monoclonal antibodies were purchased from BD Pharmingen, BioLegend, R&D Systems, or eBiosciences and used according to the manufacturers' protocols: PE conjugated anti-CD115, MHCII, Mac3, CD11b, CD31, LFA-1, F4/80, CCR2, MMR (CD206), IL-4Rα, IL–10, TNF–α, and CD64 antibodies; allophycocyanin-conjugated anti-CD45.1, CD45.2, CD62L, CD11c, SR-A1, TGF-β, IL-1β and CD11b antibodies; and PerCP-conjugated anti-Gr1 (Ly6c) and CD11b antibody. Cells were analyzed on an LSRII cytometer (BD Biosciences) using FlowJo software. In each experiment, relevant negative control groups, positive controls and single stained samples for each tissue were used to determine the populations of interest and to exclude others. In experiments using chimeric mice, the results were routinely normalized to each individual animal's percentage of chimerism measured in the blood (a normalization factor (f) was defined as f=50/ percentage of chimerism).

Multiplex cytokine analysis system.

Wild-type C57Bl/6J injured and non-injured control mice were killed at different time points after spinal cord injury. CP was isolated from lateral 3rd and 4th ventricles and pooled in groups of six, due to the limited amount of protein extracted from each individual CP. Samples from lesion sites (4mm length of spinal cord tissue) were pooled in groups of three. The excised tissues were homogenized in PBS containing protease inhibitors (1:100; P8340, Sigma). Four freeze-thaw cycles (3 minutes each) were performed to break the cell membranes. Homogenates were then centrifuged for 10 min at 500*g*, and the total protein quantities in supernatants were determined by Bradford reagent. CSF, aspirated from 12 mice in each group, was pooled (due to the limited protein amount in each single CSF sample (5 µl)) and centrifuged prior to freezing. Frozen supernatants were assayed in duplicate using Multiplex Bead-based Luminex Assays (MILLIPLEX mouse cytokine/chemokine panel or TGFβ1,2,3 MILLIPLEX kit; Millipore), performed by outsourcing to a commercial lab (American Medical Laboratories, Israel) according to the manufacturer's instructions. Results are expressed as picograms of protein per milligram of total tissue protein, for CP and lesion site samples, and as picograms of protein per milliliter for CSF samples.

Scanning electron microscopy. Animals were perfused with fixative (3% paraformaldehyde (PFA, Merck), 2% glutaraldehyde (EMS) in 0.1M Cacodylate buffer, 5nM $CaCl_2$, 1% sucrose) and the spinal cord containing the lesion site carefully dissected. The spinal cord was cut longitudinally to open and expose the central canal. After overnight post fixation in 3% PFA and 2% glutaraldehyde, samples were fixed with 1% osmium tetroxide (EMS) in 0.1M Cacodylate buffer, 5nM $CaCl_2$, and 1% sucrose for 1.5h. They were then incubated with 1% tannic acid (Merck) in DDW for 5 min, followed by incubation with 1% uranyl acetate (EMS) in DDW for 30 min. Samples were dehydrated by washing with ethanol at increasing concentrations, and then dried in a critical point dryer (CPD) (Bal-Tec 030 Leica). After mounting the samples onto aluminum stubs, they were sputter-coated with gold-palladium and imaged with a Zeiss Ultra 55 FEG SEM.

Magnetic resonance imaging. The MRI scans were performed on anesthetized mice using a 30 cm horizontal bore scanner (Biospec 47/30, Bruker, Ettlingen, Germany) at a field strength of 4.7 Tesla. A RF resonator with i.d. = 5.1 cm was used for transmission/reception. T2-weighted images of the brain in the coronal plane were obtained using a Fast-Spin-Echo (FSE) sequence, with TR =

4 s, effective TE = 56 ms, echo-train-length (ETL) = 8, averages (NEX) = 3, field-of-view (FOV) = 3.5 cm, 256x256 matrix, and slice thickness = 0.7 mm.

Near-infrared imaging. Isolated monocytes were labeled *ex-vivo* with the near infrared lipophilic carbocyanine dye, 1,1'-dioctadecyl-3,3,3',3'-tetramethylindotricarbocyanine iodide (DiR; Invitrogen), for 1h. Labeled cells were injected intravenously into Balb/c mice, approximately 4 hours after spinal cord injury. The mice were sacrificed, the skull removed, and the brain ventricles were exposed. DiR-labeled monocyte localization within organs was assessed using the IVIS 100 Series Imaging System (Xenogen), 18h after cell transplantation. The excitation (Ex) and emission (Em) filter sets were 710-760 and 810-760nm, respectively.

RNA purification, cDNA synthesis, and quantitative Real-Time PCR analysis.
For CP cell extraction and total mRNA purification, the ZR RNA microprep kit was used (Zymo Research). Reactions were performed using Power SYBR Green PCR Master Mix (Applied Biosystems) or Absolute Blue SYBER Green ROX Mix (Thermo scientific). The relative amounts of mRNA were calculated using the standard curve method and normalized to reference genes found to be best suited for our tissues, *Ppia or Gapdh.* Each sample was run in triplicate. Amplification conditions were: 50°C for 2 min, 95°C for 10 min, followed by 40 cycles of 95°C for 15 s, and 60°C for 1 min. Quantitative real-time PCR reactions were performed using the 7500 Real-Time PCR System (version 1.4; Applied Biosystems) or the StepOne software V2.2.1 (Applied Biosystems). The following primers were used:
Nt5e
Forward 5'-GCTTCAGGGAATGCAACATGGGAA-3',
Reverse 5'-ATGCCACCTCCGTTTACAATGCAC-3';
Cx3cl1
Forward 5'-ATGTGCGACAAGATGACCTCACGA-3',
Reverse 5'-TTTCTCCTTCGGGTCAGCACAGAA-3';
Madcam1
Forward 5'-AGCACTCCGTGAAGATCCTTGTGT-3',
Reverse 5'-TAGCAGGGCAAAGGAGA GACTGTT-3';
Vcam1
Forward 5'-TGTGAAGGGATTAACGAGGCTGGA-3',
Reverse 5'-CCATGTTTCGGGCACATTTCCACA-3';
Tgfb2

Forward 5'-AATTGCTGCCTTCGCCCTCTTTAC-3',

Reverse 5'-TGTACAGGCTGAGGACTTTGGTGT-3';

Icam1

Forward 5'-AGATCACATTCACGGTGCTGGCTA-3',

Reverse 5'-AGCTTTGGGATGGTAGCTGGAAGA-3';

Ccl3

Forward 5'-TTTGAAACCAGCAGCCTTTGCTCC-3',

Reverse 5'-TCAGGCATTCAGTTCCAGGTCAGT-3';

Ccl5

Forward 5'-GTGCTCCAATCTTGCAGTCGTGTT-3',

Reverse 5'-ACTTCTTCTCTGGGTTGGCACACA-3';

Gpr125

Forward 5'-ATGCTTGTGAACCTGTGCTTTC-3',

Reverse 5'-CGCTGGCATTTCTGGTCTGG-3';

Ccl19

Forward 5'-ATCGTGAAAGCCTTCCGCTACCTT-3',

Reverse 5'- CCTTCTGGTGCTGTTGCCTTTGTT-3';

Ccl21

Forward 5'- CAGGACTGCTGCCTTAAGTA-3',

Reverse 5'-GCACATAGCTCAGGCTTAGA-3';

Ppia

Forward 5'- AGCATACAGGTCCTGGCATCTTGT-3',

Reverse 5'-CAAAGACCACATGCTTGCCATCCA-3';

Vip

Forward 5'-GCAAACGAATCAGCAGCAGCATCT-3',

Reverse 5'-TCACAGCCATTTGCTTTCTGAGGC-3';

Thbs1

Forward 5'-TTGATGGATGCCTGTCCAATCCCT-3',

Reverse 5'-ACTCATCGACGTCTTTGCACTGGA-3';

CD 163

Forward GATTCAGCGACTTACAGTTTCC;

Reverse GAGGATTTCAGCAAGTCCAG;

Ppar-γ,

Forward 5′-AAGAGCTGACCCAATGGTTG-3′;

Reverse 5′-GGATCCGGCAGTTAAGATCA-3′;

Il-10

Forward TGAATTCCCTGGGTGAGAAGCTGA;

Reverse TGGCCTTGTAGACACCTTGGTCTT;

Il-6

Forward TGCAAGAGACTTCCATCCAGTTG;

Reverse TAAGCCTCCGACTTGTGAAGTGGT;

Il-1β:

Forward CCAAAAGATGAAGGGCTGCTT;

Reverse TGCTGCTGCGAGATTTGAAG;

Il-12-p35

Forward TCACCCTGTTGATGGTCACG;

Reverse AAATGAAGCTCTGCATCCTGC;

Arginase-1

Forward TCCTTAGAGATTATCGGAGCGCCT;

Reverse TTTCCAGCAGACCAGCTTTCCTCA;

Tgf-β1

Forward TACCATGCCAACTTCTGTCTGGGA;

Reverse TGTGTTGGTTGTAGAGGGCAAGGA;

Mcp-1

Forward CAT CCA CGT GTT GGC TCA;

Reverse GAT CAT CTT GCT GGT GAA TGA GT;

Tnfa

Forward GCCTCTTCTCATTCCTGCTT;

Reverse CTCCTCCACTTGGTGGTTTG;

Gapdh

Forward 5-AATGTGTCCGTCGTGGATCTGA-3;

Reverse 5-GATGCCTGCTTCACCACCTTCT-3.

Supplemental References

Auffray, C., Fogg, D., Garfa, M., Elain, G., Join-Lambert, O., Kayal, S., Sarnacki, S., Cumano, A., Lauvau, G., and Geissmann, F. (2007). Monitoring of blood vessels and tissues by a population of monocytes with patrolling behavior. Science *317*, 666-670.

Basso, D. M., Fisher, L. C., Anderson, A. J., Jakeman, L. B., McTigue, D. M., and Popovich, P. G. (2006). Basso Mouse Scale for locomotion detects differences in recovery after spinal cord injury in five common mouse strains. J Neurotrauma *23*, 635-659.
Chiang, E. Y., Hidalgo, A., Chang, J., and Frenette, P. S. (2007). Imaging receptor microdomains on leukocyte subsets in live mice. Nat Methods *4*, 219-222.
Donnelly, D. J., Longbrake, E. E., Shawler, T. M., Kigerl, K. A., Lai, W., Tovar, C. A., Ransohoff, R. M., and Popovich, P. G. (2011). Deficient CX3CR1 signaling promotes recovery after mouse spinal cord injury by limiting the recruitment and activation of Ly6Clo/iNOS+ macrophages. J Neurosci *31*, 9910-9922.
Geissmann, F., Jung, S., and Littman, D. R. (2003). Blood monocytes consist of two principal subsets with distinct migratory properties. Immunity *19*, 71-82.
Getts, D. R., Terry, R. L., Getts, M. T., Muller, M., Rana, S., Shrestha, B., Radford, J., Van Rooijen, N., Campbell, I. L., and King, N. J. (2008). Ly6c+ "inflammatory monocytes" are microglial precursors recruited in a pathogenic manner in West Nile virus encephalitis. J Exp Med *205*, 2319-2337.
Kanehiro, A., Takeda, K., Joetham, A., Tomkinson, A., Ikemura, T., Irvin, C. G., and Gelfand, E. W. (2000). Timing of administration of anti-VLA-4 differentiates airway hyperresponsiveness in the central and peripheral airways in mice. Am J Respir Crit Care Med *162*, 1132-1139.
Pereira, J. P., An, J., Xu, Y., Huang, Y., and Cyster, J. G. (2009). Cannabinoid receptor 2 mediates the retention of immature B cells in bone marrow sinusoids. Nat Immunol *10*, 403-411.
Ristevski, B., Young, A. J., Dudler, L., Cahill, R. N., Kimpton, W., Washington, E., and Hay, J. B. (2003). Tracking dendritic cells: use of an in situ method to label all blood leukocytes. Int Immunol *15*, 159-165.
Shechter, R., London, A., Varol, C., Raposo, C., Cusimano, M., Yovel, G., Rolls, A., Mack, M., Pluchino, S., Martino, G., *et al.* (2009). Infiltrating blood-derived macrophages are vital cells playing an anti-inflammatory role in recovery from spinal cord injury in mice. PLoS Med *6*, e1000113.
Ziv, Y., Avidan, H., Pluchino, S., Martino, G., and Schwartz, M. (2006). Synergy between immune cells and adult neural stem/progenitor cells promotes functional recovery from spinal cord injury. Proc Natl Acad Sci U S A *103*, 13174-13179.